A STUDY OF FRACTURE AND ARREST WHEN A FAST-PROPAGATING, BRITTLE CRACK EMANATES FROM A BRITTLE WELD INTO SOUND 3.5 % NICKEL STEEL

K. Smit, P. Bristoll and Q. Sypkens*

An investigation of fracture and arrest when a fast propagating crack runs from a local brittle weld into sound 3.5 % nickel steel plate has been conducted. Large-plate tests were carried out incorporating instrumentation to measure crack speed and changes in strain during propagation and arrest. It is concluded that crack tunnelling is a predominant factor in arrest. The fracture appearance of the tunnelled crack is quasi-brittle and the tip of the crack continues propagation at about the same speed after transition from the brittle weld into the target material. Plastic deformation only occurs after passage of the tunnelling crack. The stress intensity of the tunnelling crack may temporarily exceed the value for a static crack after penetration in the target material.

INTRODUCTION

Steel structures are designed to prevent the initiation of brittle fracture. However, an additional requirement, with respect to the capability of the steel to arrest a fast running crack, is considered to be prudent for certain structures. Such a requirement will enable the steel to arrest a fast running crack, should the remote possibility of crack initiation in a local "substandard zone" ever become a reality. The "substandard zone" is defined as an area where the code requirements for the prevention of brittle fracture are not met, notwithstanding the extensive measures taken for quality assurance during design and construction. When a brittle crack initiates in such a zone, in spite of the safety margins of the codes and a full hydrostatic test, the surrounding, sound material with as-specified toughness is then required to be able to arrest the crack.

The arrest capabilities of both 9 % and 3.5 % nickel steel and their weldments have been studied by the Koninklijke/Shell-Laboratorium, Amsterdam. The arrest capability was determined using large test plates, which were designed to simulate the case of a

* KONINKLIJKE/SHELL-LABORATORIUM, AMSTERDAM (Shell Research B.V.), Postbus 3003, 1003 AA Amsterdam, The Netherlands.

brittle crack running from a "substandard zone" into the sound material of a very large structure. The results (see Smit et al. (1) and Bristoll and De Koning (2)) were presented from the point of view of the applicability of the steels and their specifications. The work has shown that good arrest capability can be achieved for 9 % nickel steel down to -196 °C and for 3.5 % nickel steel and its weldments down to -70 °C.

This paper deals with the large-plate crack-arrest tests on 3.5 % nickel steel parent plate and is complementary to the previous paper (2) in that it concentrates on the interpretation of the dynamic behaviour of the test specimens. The test plates were instrumented with strain gauges, a crack-propagation gauge, Moiré grids and a crack-opening gauge so that it would be possible to
- determine the validity and severity of the tests
- understand the crack propagation behaviour
- translate results via fracture mechanics to other conditions.
Only the results of a selected number of tests are given. Description of all variations in instrumentation in the other tests is not feasible within the limited length of the paper, but no additional or different features have emerged from the instrumentation of these other tests. An interpretation of the measurements is given.

In particular, the phenomenon of crack tunnelling is not well understood and it is hoped that this paper will help towards the ability to model and predict the significance of such crack tunnelling in actual structural crack-arrest situations.

PROCEDURE

Design of the Test Plate

The configuration of the test plate for the crack-arrest experiments is shown in Figure 1. The substandard zone is created by a weld which is brittle at the test temperature. Brittle fracture can be initiated in a separate part of the plate after the central part of the plate has been cooled and the plate has been loaded to the test stress. The running crack is guided through the brittle weld by a single side groove which ends at the end of the brittle weld. The transition between the brittle weld and the target material was sharp and straight.

The considerations which led to the above design of the test plate and the choice of its dimensions are given in reference (2).

Materials

The material tested was controlled rolled, quenched and tempered 3.5 % nickel steel plate, thicknesses 12 and 22 mm. The chemical composition and the tensile properties of the plates are

given in Table 1. The 40 J transition temperature for longitudinal Charpy-V impact specimens was -160 and -145 °C respectively. The Pellini Nil-Ductility Temperature of the thick plate was -120 °C.

TABLE 1 - Chemical Composition and Mechanical Properties of Test Material

t, mm	% C	% Si	% Mn	% P	% S	% Ni
12	0.08	0.25	0.55	0.010	0.001	3.56
22	0.08	0.24	0.55	0.008	0.001	3.54

t, mm	Yield strength MPa		Tensile strength MPa		Elongation %		Reduction in area %
	at 20 °C	at -100 °C	at 20 °C	at -100 °C	at 20 °C	at -100 °C	at -100 °C
12	460	530	590	700	37	33	78
22	440	480	560	650	37	33	80

Instrumentation of the Test Plates

The purpose of the instrumentation was:
- to measure the crack speed in the brittle weld; this is considered an important parameter in terms of the severity of the test
- to determine the crack speed in the target material and the moment of arrest
- to measure the changes in strain at the plate boundaries in order to demonstrate that, up to the moment of arrest, the plate behaves as an infinite plate. This avoids complex analysis in cases where the results of the tests are to be used to predict the arrest of cracks in large thin shells
- to determine the development of plasticity, necking and tearing and hence to ascertain their role in arrest
- to verify dynamic finite-element calculations of the strain distribution during fracture against the measured strain records at various positions.

Crack-propagation gauges. Crack-propagation gauges were inserted at the non-grooved side of the brittle welds. In most tests the gauges consisted of 12 equidistant conducting wires across the weld. The moment of failure of the first wire, which was located at the transition from starter plate to test plate, has been taken as time zero. The moment of failure of the wires was recorded with 1 μs accuracy.

Strain gauges. An array of strain gauges was inserted in the target area at the end of the brittle weld to monitor transient strain variations during propagation and arrest. The strain gauges are designated by xsgy, x representing the number of the test and y the number of the gauge as indicated in Figure 2. Strain gauges were also inserted near the plate boundaries (gauges a and b in Figure 1) to establish when and how the stresses at the boundaries would change in response to the fracture process. The recording range of the strain gauges was +/- 12.000 microstrain ($\mu\epsilon$). The system of strain gauges, amplifier and recorder is capable of recording strain variations with a rate of change up to 2500 $\mu\epsilon/\mu$s.

Moiré grid. In selected tests a Moiré grid was fitted to the plate surface in the target area at the end of the brittle weld. The lines of the Moiré grid (20 lines/mm) were perpendicular to the loading direction. The Moiré pattern was photographed after the plate, with the loading removed, had been warmed up to room temperature.

Crack-opening gauge. A crack-opening gauge has been developed which measures the opening of the crack in the brittle weld at two positions, 50 mm apart. The gauge incorporates two pairs of light sources, which are tightly screwed into the plate; for each pair one on either side of the crack. The displacements between the light sources are monitored with photo-sensitive detectors.

FRACTOGRAPHY AND TEST RESULTS

The test plates were cooled after the test to about -170 °C and broken open. A typical fracture surface is shown in Figure 3. In all tests the crack penetrated into the target area by tunnelling.

The crack emanated generally from the brittle weld at an angle of between 0 and 30° to the centre line of the brittle weld. Further down into the test material the crack resumed the direction of crack propagation perpendicular to the load applied. At the end of the brittle weld there was an initial tendency towards crack branching in most of the tests.

The features on the fracture surface indicate that the crack front reached the target area first on the side of the plate with the side groove and that crack tunnelling developed from that point into the target material.

The fracture mode of the tunnelled crack in the target area was quasi-cleavage, as was the fracture mode in the brittle weld. In comparison with the fracture in the brittle weld, the fracture surface of the tunnelled crack was rougher, with clear chevron markings; at high magnification (greater than 1000x) the brittle facets were found to be larger and less ductile features were present.

The amount of deformation of the ligaments of the tunnelled crack at the end of the test varied considerably. The ligaments in Figure 3 are hardly stretched; a thin, shiny stretched zone can be seen as a contour of the tunnelled crack. In contrast, thin ligaments of cracks which had tunnelled over a relatively long distance into the target material were found to be stretched until the cross-section of the ligament had been reduced to a line contact just prior to separation. It is noted that only the ligaments in test 2, which fractured completely, and a very short part of a ligament in test 12 (Δa = 141 mm) had fractured under 45° shear.

The test conditions and the test results in terms of penetration into the target material are given in Table 2.

TABLE 2 - Test Conditions and Results

t mm	T °C	No.	σ_A MPa	L mm	Δa mm	$\dot{a}$ m/s	K_S MPa$\sqrt{mm}$	K_D MPa$\sqrt{mm}$
22.5	-90	2	385	115	∞*	1500	7320	4220
22.7	-90	4	263	120	135	-	5110	-
22.3	-91	9	194	122	5	588	3800	3220
22.5	-81	8	385	118	56	940	7410	5540
22.3	-79	10	389	79	36	1395	6130	3740
22.5	-83	12	392	125	141	1365	7770	4820
21.8	-82	13**	405	115	58	1200	7700	5160
22.2	-70	5	391	120	39	1285	7590	4900
22.5	-70	6	385	75	29	985	5910	4340
12.2	-90	1	380	120	31	2000	7380	3010
11.8	-101	15	401	117	21	1720	7690	3880
11.9	-110	11	387	115	66	1745	7360	3650

* no arrest occurred
** preloaded at room temperature to 308 MPa

CRACK SPEED AND STRAIN MEASUREMENTS

Crack Speed Measurement in the Brittle Weld

The wires of the crack-propagation gauge have been assumed to break at the moment of passage of the crack tip, because no visible surface plasticity developed during crack propagation through the brittle weld. It is noted that the crack-propagation gauge recorded the passage of the trailing end of the crack front (see previous section).

The crack speed was fairly constant along the brittle weld. Some acceleration often occurred at the beginning and near the end of the brittle weld. The position of the trailing crack tip at the non-grooved surface versus time is given for tests 11 and 13 in Figure 4. The average crack speed in each test is given in Table 2. For tests with nominally the same test conditions the crack speed is scattered, but it is clear that in thin plates the crack speed is higher than in thick plates and that lessening the applied stress reduced the crack speed by about the same factor.

Strain Measurements in the Target Area

The response of a strain gauge to the penetration of the crack into the target area is dependent on:
- the distance of the strain gauge from the crack path
- the distance of the strain gauge from both the end of the brittle weld and the position of arrest
- the width of the ligaments of the tunnelled crack and the amount of stretching of these ligaments
- the uniformity of the fracture propagation.

These factors varied from test to test, making interpretation of the strain records complicated.

For the sake of brevity only the following strain-gauge records have been selected for presentation in this paper:
- 5 records of test 12 (Figure 5, A)
- some characteristic records of several tests (Figure 5, B).

In most tests, strain gauge 6, which was close to the end of the brittle weld, responded with a relatively sharp peak to the passing of the crack. This was immediately followed by relaxation, when the crack penetrated into the target area, to below the level of strain at the start of the test. The maximum increase in strain at the peak (h) is given in Table 3.

TABLE 3 - Data obtained from Instrumentation

No.	sg/a	sg/b	t(a) μs	c.o.* mm	$\dot{a}$ m/s	h $\mu\epsilon$	K(p) MPa$\sqrt{m}$	K(p)/K_S
8	120	180	159	-	940	-		
9	124	330	206	1.0	588	600	3270	0.86
10	128	180	68	1.7	1395	550	5160	0.84
11	144	192	99	4.3	1745	1400	6970	0.95
12	144	192	189	-	1365	1200	6590	0.85
13	-	200	137	3.2	1200	1000	6290	0.82
15	135	180	78	4.7	1720	950	6140	0.80

* after >20.000 μs

Strain gauges which were located just outside the plastically deformed band alongside the crack responded to the passing of the crack with an elastic double peak above the level of strain at the start of the test (e.g. 11sg8 in Figure 5, B). The "first peak" was only observed when tunnelled cracks had very thin ligaments. For cracks with wider ligaments only a single peak was observed, namely the "second peak"; the "first peak" was then reduced in height to such an extent that it was observed not as a separate peak but as a small "deviation" in the upward slope of the "second peak".

The single peaks (e.g. 12sg8 and 12sg10 in Figure 5, A) were wider and also higher than for strain gauge 6; in test 12 the heights of the peaks for strain gauges 6 to 10 were 1200, 1700, 2250, 1600 and 1500 $\mu\epsilon$. After the peak, the strains in test 12 (Δa = 141 mm) returned to nearly the level of strain at the start of the test for about 1000 μs before relaxation of the overall stresses started to occur. In most other tests, the crack only penetrated into the target area over a small distance and as a result the development of the peak was interrupted by the arrest.

A small "deviation" in the slope to high strains is also generally observed for strain gauges located within the band along the crack where plasticity developed (e.g. 12sg3 and 13sg3 in Figure 5, B). However, unlike the strain gauges outside the band of plastic deformation, the strains increased to well within the plastic regime immediately after the "deviation". The strain rate after the "deviation" is remarkably constant for tests 11, 12, 13 and 15, being in the range of 100 to 140 $\mu\epsilon/\mu$s. For test 10, with a shorter brittle weld (79 mm), the strain rate was about 46 $\mu\epsilon/\mu$s.

The moments at which either the maximum of the "first peak" (in case of a double peak) or the "deviation" was reached have been taken as the moment of passage of the tunnelling crack tip. These times are given in Figure 4 for tests 11 and 13, together with the moments at which the crack passed the wires of the crack-propagation gauge. The apparent discontinuity in crack propagation at the end of the brittle weld may be an artifact resulting from a different moment of response of the crack-propagation gauge and the strain gauge relative to the position of the crack tip and also from the shape of the crack front in the brittle weld (see section "Fractography and Test Results" above).

Changes in strain beyond 300 μs were greatly dependent on the position of the strain gauge relative to the point of arrest; strain gauges in front of the crack tip continued to register an increase, whereas strain gauges well behind the crack tip recorded elastic relaxation.

Strain Records of Gauges near the Plate Boundaries

Typical records of strain gauges "a" and "b" (Figure 1) are given in Figure 6.

The first drop in strain always occurred at the strain gauges "a". The moment of first disturbance in each test is given in Table 3.

At strain gauge "a" there was only a slight (<11 %) drop in strain after the initial oscillations had decayed; at gauge "b", though, the drop was considerable ($\leqslant$ 89 %). The drop in strain did not correlate with crack length. The moment at which the lower

level of strain was first reached was in the range 2000 to 3800 μs.

Moiré Deformation Pattern

An example of a deformation pattern revealed by Moiré is given in Figure 7. The narrow band of plastic deformation along the tunnelled crack widened towards the crack tip. Ahead of the crack tip the plastic zone extended as a narrow tongue into the plate. The plastic zone widened considerably just ahead of the crack tip in tests where considerable stretching of the ligaments occurred, to form a pear-shaped plastic zone.

Crack Opening

An example of a crack-opening record 35 mm from the transition between test and starter plate is given in Figure 6. Generally, the crack opened in the first 200 μs to just over half the crack opening that was finally attained. Thereafter, the crack opened more slowly, in a period ranging from 1000 to 20.000 μs. The crack opening after more than 20.000 μs in each test is given in Table 3.

DYNAMIC FINITE-ELEMENT CALCULATIONS

A strain analysis was made of plate 13 during crack propagation using a dynamic, elastic-plastic finite-element programme (Vo and Luxmoore (3)). The input data for the analysis were: a) plate geometry, b) applied stress, c) assumed residual stress distribution associated with the brittle weld, d) crack speed as a function of crack length and e) a bilinear stress-strain curve approximation for the 3.5 % nickel steel. Strains at the positions of the strain gauges 1 to 5 and 7 to 14 could not be predicted accurately, because the complex nature of crack propagation into the target material was not modelled. In contrast, the calculated strain peak of strain gauge 6, which records material response before tunnelling, was 1000 $\mu\epsilon$, which agrees with the measured value as in Table 3. The stress intensity factor which was calculated for the crack passing through the final part of the brittle weld was 5190 MPa$\sqrt{\text{mm}}$.

DISCUSSION

Propagation and Arrest of the Crack in the Test Material

The brittle, quasi-cleavage fracture modes of both the brittle weld and the tunnelled crack indicate that no dramatic change in crack speed occurred on entry into the target material. This is in line with the observation from Figure 4 that the crack speed obtained for the target material is similar to the crack speed in the brittle weld, if the response of "first peak" and "deviation" in the strain-gauge records are interpreted as the passing of the crack.

An estimate of the moment of arrest, t(a), has been obtained by adding to the time of the peak of strain gauge 6 the time that the crack tip needs to travel from the position of strain gauge 6 to the full depth of penetration at a speed equal to the crack speed in the brittle weld. Values for t(a) are given in Table 3.

In some tests a sudden change in the rate of decay for strain for gauge 6 occurred shortly after t(a), but in other tests such a change was difficult to determine and therefore unreliable as an indication of arrest.

Plate Geometry

Changes in strain at the plate boundaries can only influence the arrest after they have been transmitted back to the crack. The maximum speed of transmission is the longitudinal wave speed (6000 m/s). For the size of plate involved the first change in strain at the loaded boundaries as a result of the fracture process can only affect arrest 140 μs later.

Initially (2) it was arbitrarily considered that for a valid arrest, in view of boundary interaction, the crack penetration should be less than 3 times the plate thickness (t). However, from Table 3 it can be seen that even the arrests in tests 11 and 12, where crack penetrations were beyond 3t, may be considered as independent of the size of the plate.

Critical Conditions for Arrest

The boundary between arrest and no-arrest conditions in terms of applied stress and temperature has been given as an arrest-transition curve in reference (2). A possible influence of the length of the brittle weld is ignored in this transition curve.

Alternatively, the stress intensity factor for a crack as long as the brittle weld may be considered as a parameter for the severity of the test. The test plate can be considered representative for a centre-cracked, infinite plate because the crack does not experience any influence of the plate boundaries before arrest. In particular, the larger crack openings which are typical for an edge-cracked configuration cannot occur before the arrests. Therefore, the static stress intensity factor $K_S = \sigma_A\sqrt{\pi a}$ for a centre crack in an infinite plate is used for analysing arrest conditions in these tests. The values for K_S at the end of the brittle weld are given in Table 2.

The crack penetration in the test material (Δa) is found to be dependent on K_S for small amounts of tunnelling as indicated in Figure 8. A similar dependence of crack penetration on the static stress intensity factor has been reported for 9 % nickel steel (Watanabe and Yamagata (4)).

An influence of crack speed in the brittle weld is indicated by tests 8, 12 and 13, where increasing depth of penetration was found for increasing crack speed. However, small variation in other test parameters (K_S and T) could just as well account for the variation in depth of penetration observed.

Stress Intensity Factor for the Propagating Crack

For a fast propagating crack the stress intensity factor should be corrected for crack speed. A dynamic stress intensity factor (K_D) has been calculated using the following expression (Sih (5)):

$$K_D/K_S = (C_R-\dot{a})/C_R\ (1-\dot{a}/C_L) \qquad (1)$$

with C_R = Rayleigh wave speed (m/s)
C_L = longitudinal wave speed (m/s) and
$\dot{a}$ = crack speed (m/s).

For 3.5 % nickel steel C_R and C_L are about 3000 and 6000 m/s respectively. The values for K_D at the end of the brittle weld are given in Table 2. It was found that the dynamic finite-element analysis of test 13 gave nearly the same value as obtained with the above calculation.

Strain gauges 6 in all tests gave a narrow peak associated with the passage of the crack through the end of the brittle weld. According to Westergaard's distribution of stresses around a crack tip the maximum stress in the loading direction σ_{yy} (max) when the crack passes at a distance s is related to the stress intensity factor K by:

$$\sigma_{yy}\ (\max) = 1.235\ K/\sqrt{2\ \pi\ s} \qquad (2)$$

σ_{yy} (max) can be obtained from the records of the strain gauges 6 by

$$\sigma_{yy}\ (\max) = \sigma_A + E.h$$

with σ_A = applied stress
E = modulus of elasticity and
h = height of the peak in the strain record (Table 3)

The values of the stress intensity factor derived in this way, K(p), are given in Table 3. K(p) was always significantly greater than K_D. The ratio of K(p) to K_S (see Table 3) was fairly constant (except for test 11) and independent of crack speed, which seems to contradict equation (1).

The Stress Intensity Factor of the Tunnelling Crack

An effective stress intensity factor for the tunnelling crack may be calculated by equation (2) from the height of the peaks in the records of the strain gauges along the crack path. For gauges 6 to 10 of test 12 these peaks are well developed. Using the actual distance to the crack path, the values for K(p) are 6590, 9120, 10820, 9110 and 8610 MPa$\sqrt{mm}$ respectively. For a crack reaching the same depth as the position of the strain gauge the values for $K_S = \sigma_A\sqrt{\pi\, a}$ are 7770, 8150, 8510, 8860 and 9190 MPA$\sqrt{mm}$. This indicates that the effective stress intensity factor of the tunnelling crack will temporarily exceed the stress intensity of a static crack in an infinite plate by just over 20 % once the crack enters the target material and becomes progressively arrested to form a tunnelled crack. This overshoot of the static value is significantly more than the 8 % that has been calculated for a straight-fronted crack (Achenbach and Tolikas (6)).

The increase of K(p) after the crack has left the brittle weld is thought to be caused by the decelerations which result when the crack is arrested progressively along its crack front while tunnelling. At some point K(p) decays towards the level of K for a tunnelled crack. The latter is lower than K for a straight-fronted crack because of the restraining influence of the ligaments on crack opening. This means that the dynamic increase of K during tunnelling exceeds the previously mentioned 20 % because K for a tunnelling crack is smaller than for a straight-fronted crack. This large overshoot of K must be borne in mind when attempting to predict the occurrence of arrest from small-scale fracture-mechanics tests.

Plastic Deformation during and after Arrest

The records of the crack-opening gauges and the strain gauges indicate that plastic deformation in a band alongside the crack does not occur prior to passage of the crack tip, but starts shortly after the tip of the tunnelling crack has passed. The deformation rate is related to K_S, as is the initial crack opening that is attained. The initial stage of plastic deformation and crack opening is considered typical for centre cracks. The subsequent stage of more gradual deformation results from further crack opening, when the plate starts to respond as an edge-cracked plate.

Plastic deformation of the ligaments of the tunnelled crack results in necking. From the tensile tests it has been seen that the steel develops a very high reduction in area before fracture. This indicates a high potential for necking and may explain the fact that in most tests shear fracture of the ligaments did not occur. Shear fractures only developed in tests with long crack penetrations where large strains could develop.

CONCLUSIONS

1) Crack tunnelling was found to be a predominant factor in arrest of cracks in 3.5 % nickel steel. No plastic deformation was found to occur close to the crack path prior to passage of the tunnelling crack. The speed of the tunnelling crack was about the same as the crack speed in the brittle weld. Immediately after the passage of the crack, rapid plastic straining and crack opening occurred to a level related to the stress intensity of the crack, as if it were in an infinite plate. Thereafter the cracks opened more slowly under influence of the edge-cracked geometry of the plate.

2) Shear fracture of the ligaments of the tunnelled crack did not occur except for long crack penetrations because of the high potential for necking of the steel.

3) The size of the test plates was sufficiently large to avoid any influence of the plate boundaries on propagation and arrest. As a consequence the test results are representative for centre cracks in infinite plates.

4) The stress intensity of the tunnelling crack, once it starts tunnelling into the target material, significantly exceeds the stress intensity for a static crack of the same length.

5) The significant increase of K at the moment crack tunnelling begins must be taken into account when predicting crack arrest on the basis of small-scale fracture-mechanics tests and dynamic analysis.

SYMBOLS USED

Δa	= crack penetration in target material (mm)
$\dot{a}$	= crack velocity in brittle weld (m/s)
C_L	= longitudinal wave speed (m/s)
C_R	= Rayleigh wave speed (m/s)
c.o.	= crack opening (mm)
E	= modulus of elasticity (MPa)
h	= height of peak in record of strain gauge 6 ($\mu\epsilon$)
K	= stress intensity factor
K_D	= dynamic stress intensity factor (MPa$\sqrt{mm}$)
K(p)	= stress intensity factor derived from strain record (MPa$\sqrt{mm}$)
K_S	= static stress intensity factor (MPa$\sqrt{mm}$)
L	= length of brittle weld (mm)
No.	= test reference number
sg/a	= moment of first change in strain for strain gauge a (μs)
sg/b	= moment of first change in strain for strain gauge b (μs)

Symbols Used (contd.)

t	= plate thickness (mm)
T	= test temperature (^oC)
$t(a)$	= moment of arrest (μs)
$\mu\epsilon$	= microstrain
σ_A	= applied stress (MPa)
σ_{yy} (max)	= maximum stress in the loading direction (MPa)

REFERENCES

(1) Smit, K., Bristoll, P. and Stannard, D., "Steel Selection for Cryogenic Application: Ability of a Material to Arrest a Propagating Brittle Crack", Proceedings of the Conference on "Transport and Storage of LPG & LNG", Brugge, Belgium, 1984. Publisher Koninklijke Vlaamse Ingenieursvereniging, Antwerp, Belgium, Vol. 1, pp. 145-154.

(2) Bristoll, P. and De Koning, A.C., "Crack Arrest Capability of a Controlled Rolled, Quenched and Tempered 3.5 % Nickel Steel", Proceedings of the International Symposium on "Fracture-safe Designs for Large Storage Tanks", Newcastle, UK, April 1986.

(3) Vo, T. and Luxmoore, A.R., University College of Swansea, "Finite Element Analysis of Dynamic Cracking in Shell Wide-plate Specimens". Private communication, January 1986.

(4) Watanabe, I. and Yamagata, S., "Propagation and Arrest of Brittle Crack in 9 % Nickel Steel Structures for LNG Service", Proceedings of the Conference on "Transport and Storage of LPG & LNG", Brugge, Belgium, 1984. Publisher Koninklijke Vlaamse Ingenieursvereniging, Antwerp, Belgium, Vol. 1, pp. 127-136.

(5) Sih, G.C., "Mechanics of Fracture 4. Elastodynamic Crack Problems", Noordhoff International Publishing, Leiden, The Netherlands, 1977.

(6) Achenbach, J.D. and Tolikas, P.K., "Elastodynamic Effects on Crack Arrest", ASTM STP 627, "Fast Fracture and Crack Arrest", USA, 1976.

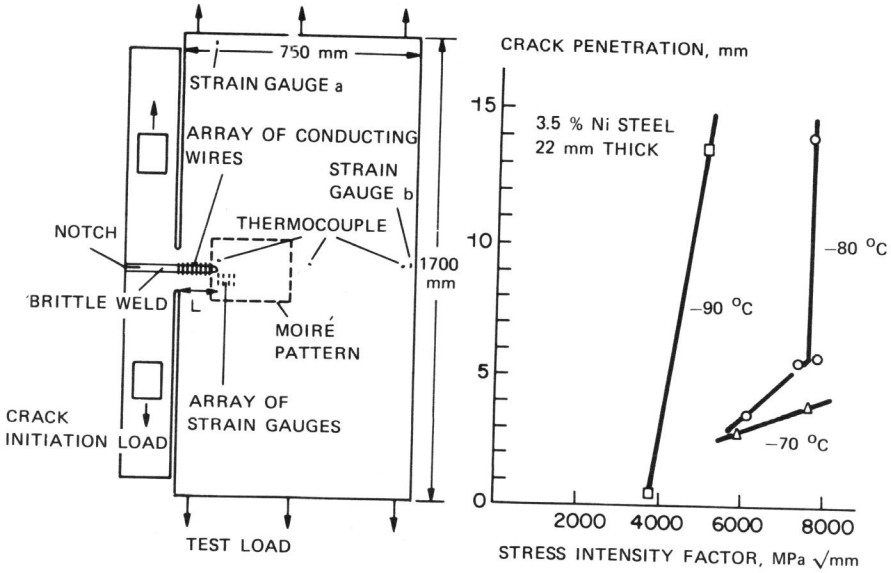

Figure 1 Design of test plate for crack-arrest tests

Figure 8 Crack penetration in test material

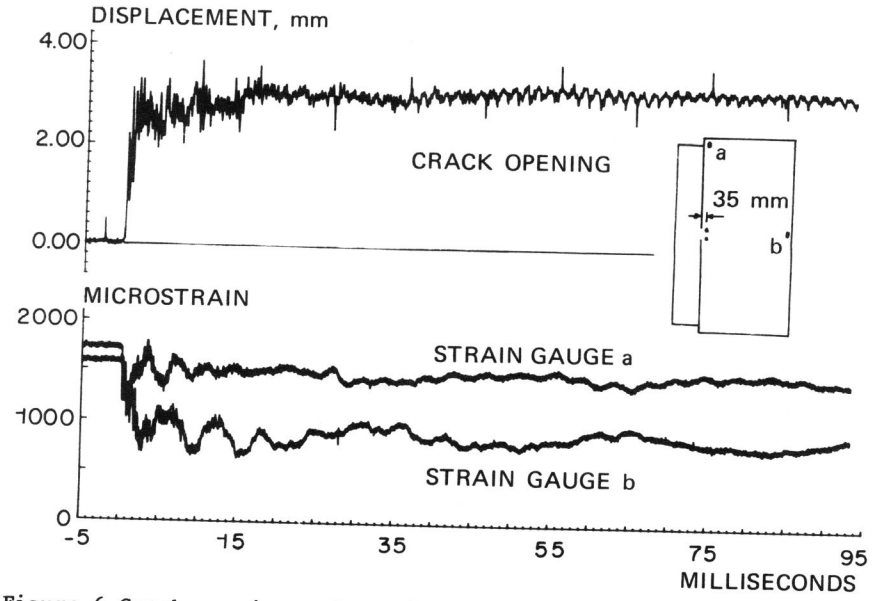

Figure 6 Crack opening and strain recorded in test 13

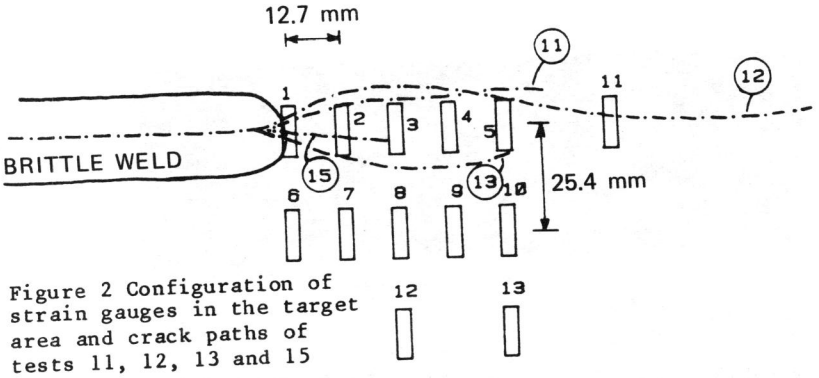

Figure 2 Configuration of strain gauges in the target area and crack paths of tests 11, 12, 13 and 15

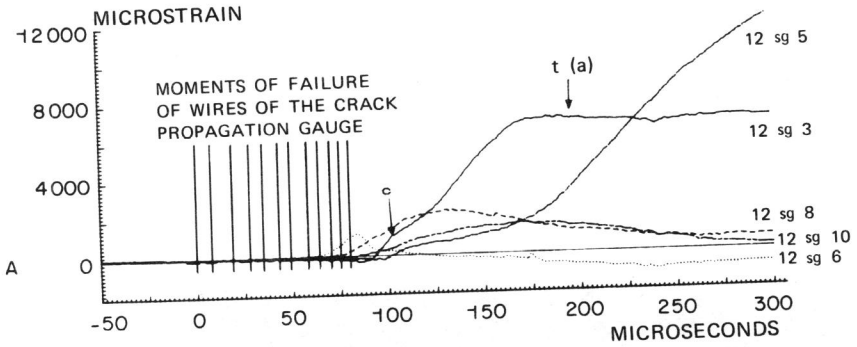

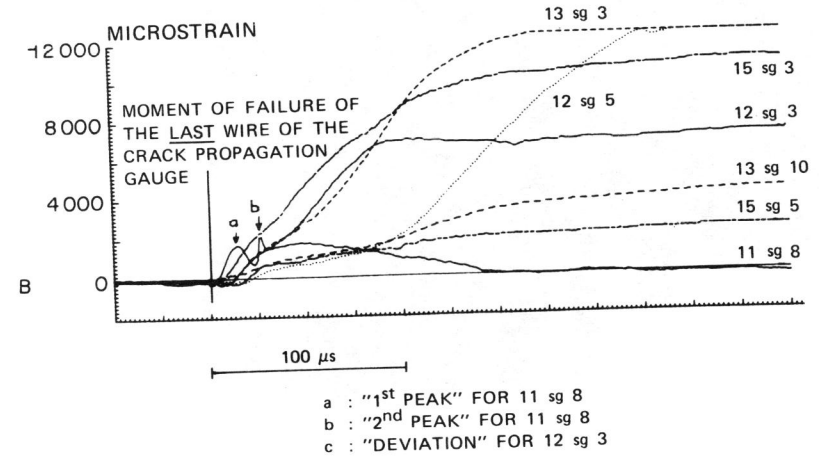

Figure 5 Selected strain-gauge records of various tests

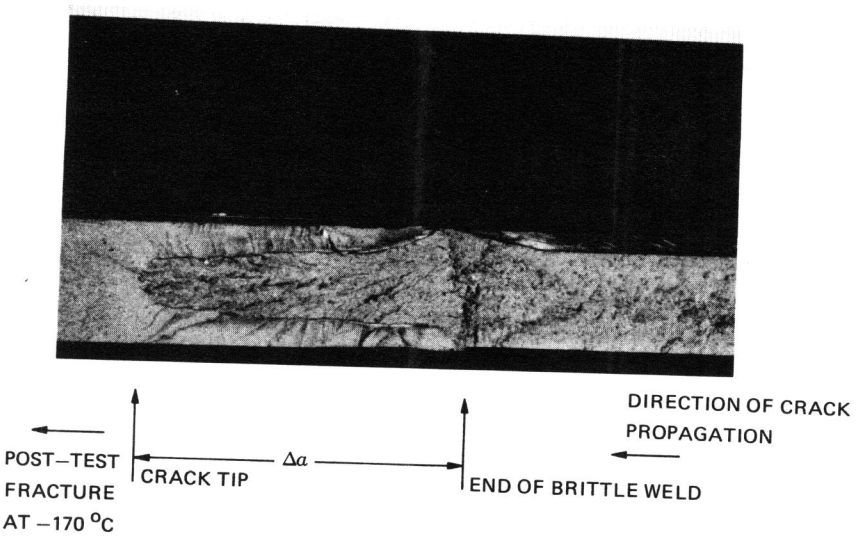

Figure 3 Fracture surface in test 13

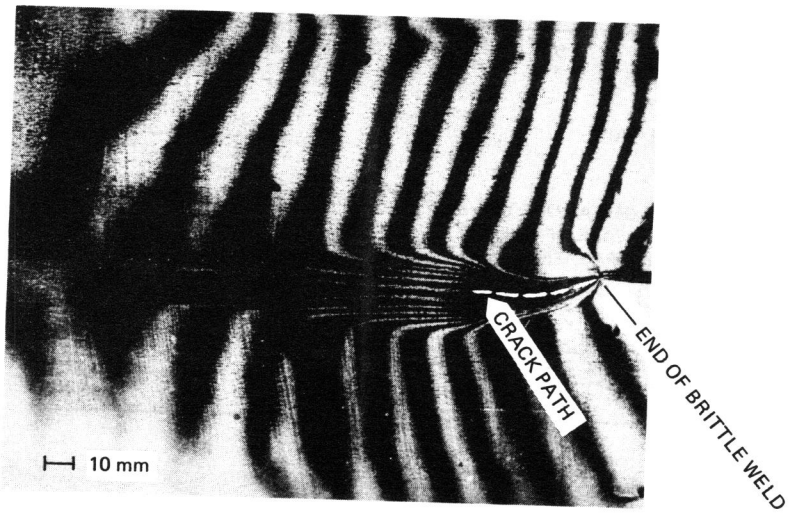

Figure 7 Moiré pattern of plastic zone along and ahead of crack in test 13

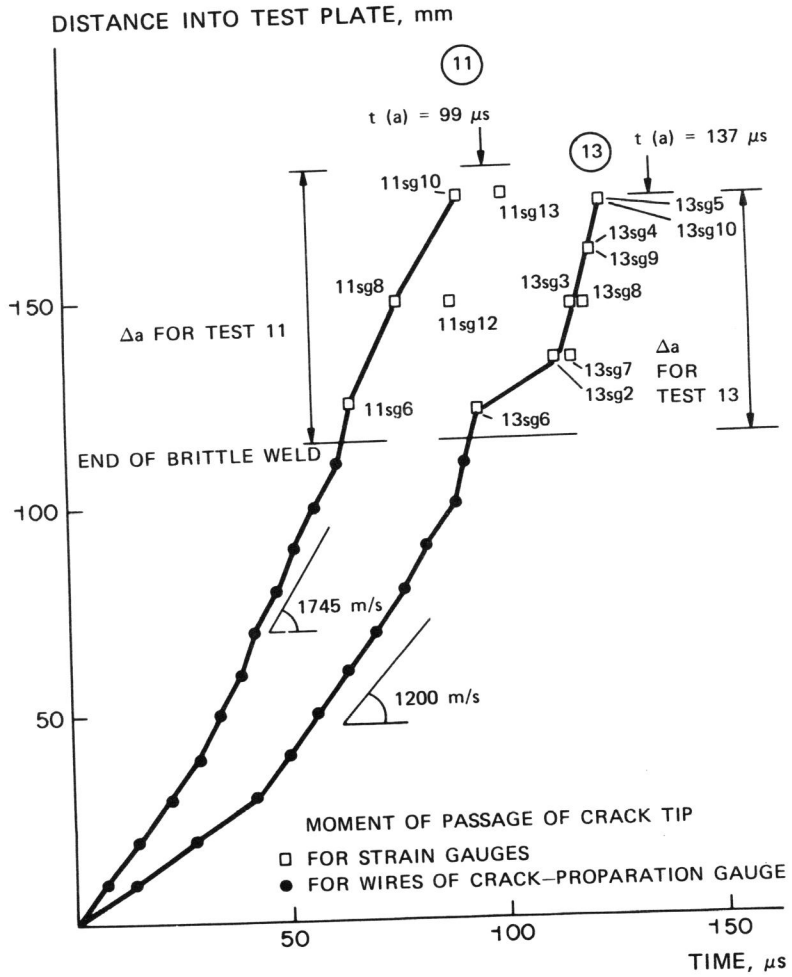

Figure 4 Crack tip position as recorded by gauges vs. time